

Cause Analysis for Wall Thinning of Small-Bore Piping in Nuclear Power Plant by ToSPACE, FLUENT and Theoretical Evaluation

Kyeongmo Hwang, Ilsu So, Hyukki Seo

KEPCO E&C, Gimcheon-si, Korea

Email: hkm@kepc0-enc.com

How to cite this paper: Hwang, K., So, I. and Seo, H. (2022) Cause Analysis for Wall Thinning of Small-Bore Piping in Nuclear Power Plant by ToSPACE, FLUENT and Theoretical Evaluation. *World Journal of Nuclear Science and Technology*, 12, 101-112. <https://doi.org/10.4236/wjnst.2022.123009>

Received: September 21, 2022

Accepted: July 28, 2022

Published: July 31, 2022

Copyright © 2022 by author(s) and Scientific Research Publishing Inc.

This work is licensed under the Creative Commons Attribution International License (CC BY 4.0).

<http://creativecommons.org/licenses/by/4.0/>



Open Access

Abstract

It has been known that FAC, LDIE, cavitation and flashing are the damage mechanisms that can cause the pipe thickness of the secondary system of nuclear power plants thinner. Severe wall thinning was found in the MSR drain pipes at a Korean nuclear power plant a decade ago, and all the affected pipes were replaced with low alloy steel with higher chromium contents. Therefore, this study was conducted to reduce the possibility of similar thinning cases that may occur in the future by identifying the exact cause of thinning. ToSPACE and FLUENT codes and theoretical evaluation method were applied to analyze the causes of thinning. ToSPACE and FLUENT analyses and theoretical evaluation including all the operating conditions show a relatively large pressure drop and a pressure lower than the saturated vapor pressure in common at the end of the pipe entering the condenser. This means that flashing occurs at the end of the pipe under all operating conditions, and the effect can be greater than that of other parts. As a result, since severe wall thinning occurred at the end of the pipeline entering the condenser, it was evaluated that flashing by the high-velocity two-phase fluid was the direct cause of the wall thinning in the MSR drain pipes. The results of this study will contribute to establishing appropriate countermeasures in the event of pipe wall thinning in the future.

Keywords

Wall Thinning, ToSPACE, FLUENT, Flashing, Cavitation

1. Introduction

Damage mechanisms that cause the wall thinning of the secondary system's pipes of nuclear power plants include flow-accelerated corrosion (FAC), liquid droplet

impingement erosion (LDIE), cavitation, flashing, etc. FAC means a corrosion phenomenon induced by fluid flow. LDIE means a phenomenon in which droplets entrained in steam flow erode the base material by continuously colliding with the pipe surface. Cavitation means a phenomenon in which the surface of the pipe is eroded by the burst pressure of cavities. The cavities inside pipe form when the operating pressure falls below the saturated vapor pressure. Flashing means a phenomenon in which the surface of a pipe is eroded by fast flow that is generated when the pressure inside pipes is not recovered after operating pressure falls below the saturated vapor pressure.

When the pipe thickness of the moisture separate re-heater (MSR) drain system installed at a Korean nuclear power plant was measured more than 10 years ago, severe wall thinning was found in the small bore pipes installed to send the condensed water from the moisture separate re-heater (MSR) to the condenser. It was judged then that the pipes had been damaged by FAC, and the thinned carbon steel pipes were replaced with low-alloy steel material with high chromium contents. However, in the case of erosion damage, low alloy steel with high chromium content is not considered to be more resistant than carbon steel based on EPRI report [1] and studies of Hwang *et al.* [2] [3]. EPRI report describes that materials resistant to FAC may not provide much additional protection from erosion. The experimental studies of Hwang *et al.* describe the mass loss rate of A106 B (carbon steel) was greater than that of A335 P22 (low alloy steel) in the initial stage of experiment, but after a critical period of time, the mass loss rate of A335 P22 was greater than that of A106 B.

This study was conducted to reduce the possibility of similar thinning cases that may occur in the future by identifying the exact cause of thinning as described above. Flow behavior was analyzed using ToSPACE and FLUENT codes for clarifying the cause of thinning, and at the same time, cavitation and flashing were evaluated based on Tullis theory.

2. Status of Design, Operation and Damage

2.1. Design & Operating Conditions

The location of wall thinning to be analyzed is a small bore pipe for transferring water condensed in the MSR to the condenser. **Figure 1** shows a schematic diagram of the MSR drain system including the thinned pipe. The main pipe where an isolation valve is installed is 1.5-inch schedule 80 (5.08 mm thick), and its design pressure and temperature are 758.23 kPa and 176.67°C, respectively. The orifice bypass piping is 1.0-inch schedule 80 (4.55 mm thick). The isolation valve is opened until 15% power after plant startup, while the valve is opened from 15% to 0% power after shutdown. That is, the isolation valve is closed during normal operation. On the other hand, the orifice piping is always opened.

2.2. Damage Feature

The location where the thinning occurred is the pipe indicated by the arrow in

Figure 1. This location is connected to a 20-inch header at the front of the condenser and is a bend pipe with a radius of curvature 5 far from the MSR. **Figure 2** illustrates the inner surface photos of the thinned pipe. Unlike flow-accelerated corrosion damage, which is usually thinned in a smooth shape, the thinned area is roughly damaged, such as scratched with a nail. The minimum-measured thickness of the pipe is 1.32 mm, which is corresponding to 74% of the nominal wall thickness (5.08 mm).

3. Cause Analysis for Wall Thinning

3.1. Cause Analysis Using ToSPACE

The causes of thinning were analyzed using the thermal hydraulic analysis function of ToSPACE [4]. The scope of modelling for performing thermal hydraulic analysis is from the two pipes in front of the orifice and valve to the thinned location connected to the header pipe as shown in **Figure 1**. **Figure 3** shows the pipeline model configured with ToSPACE, which consists of a total of 42 individual components, such as elbow, tee, pipe, etc. The analysis was performed on two cases: (Case 1) normal operating condition in which the fluid flows only through the pipeline installed with the orifice, whereas (Case 2) low power condition in which the fluid flows through both the pipelines installed with the valve and the orifice. **Table 1** shows the thermal hydraulic analysis conditions using ToSPACE. In Case 2, the inlet boundary conditions of the two pipelines are same.

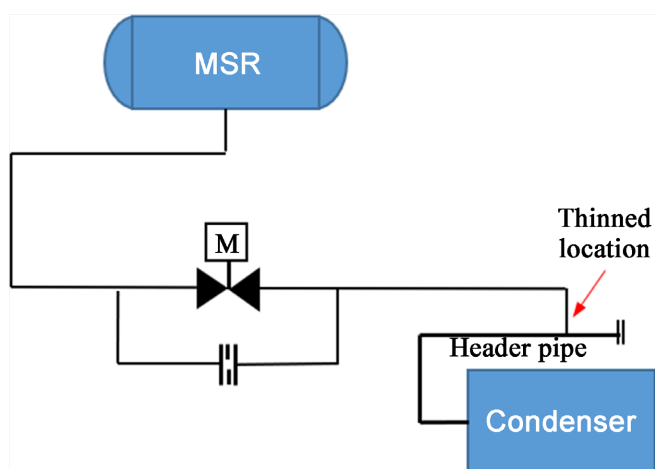


Figure 1. Schematic diagram.



Figure 2. Inner surface photos of damaged pipes.

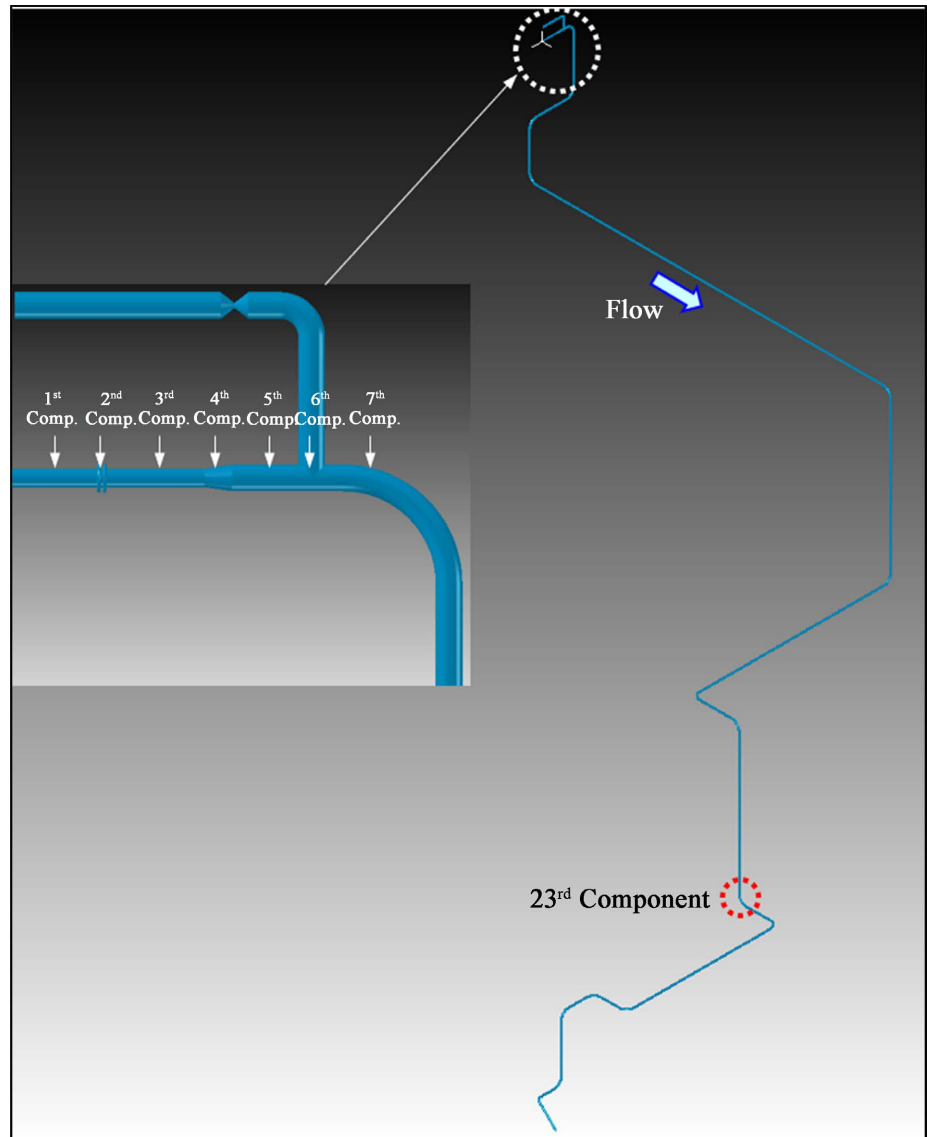


Figure 3. Analysis model using ToSPACE.

Table 1. Boundary conditions for thermal hydraulic analysis using ToSPACE.

Analysis Cases	Inlet		Outlet	Remarks
	Pressure, kPa	Enthalpy, kcal/kg	Pressure, kPa	
Case 1	683.24	171.50	26.19	Normal operation
Case 2	67.21	116.67	26.19	Low power operation during startup & shutdown

Figure 4 shows the steam quality and flow velocity inside the individual components constituting the pipeline as the analysis results for Case 1. **Figure 5** shows the operating pressure and saturated vapor pressure. Here, the pipeline where the valve is installed was excluded from the graph because of no fluid flows therein. In addition, since ToSPACE considers heat transfer to the outside at-

mosphere of the pipeline, the temperature and the saturated vapor pressure change accordingly. It is illustrated in **Figure 4** that the steam quality gradually increases as it goes downstream of the pipeline, and accordingly, the flow velocity increases. In **Figure 5**, it can be seen that the operating pressure after passing through the orifice rapidly decreases below the saturated vapor pressure and is maintained up to the pipeline outlet. From this fact, it can be seen that flashing

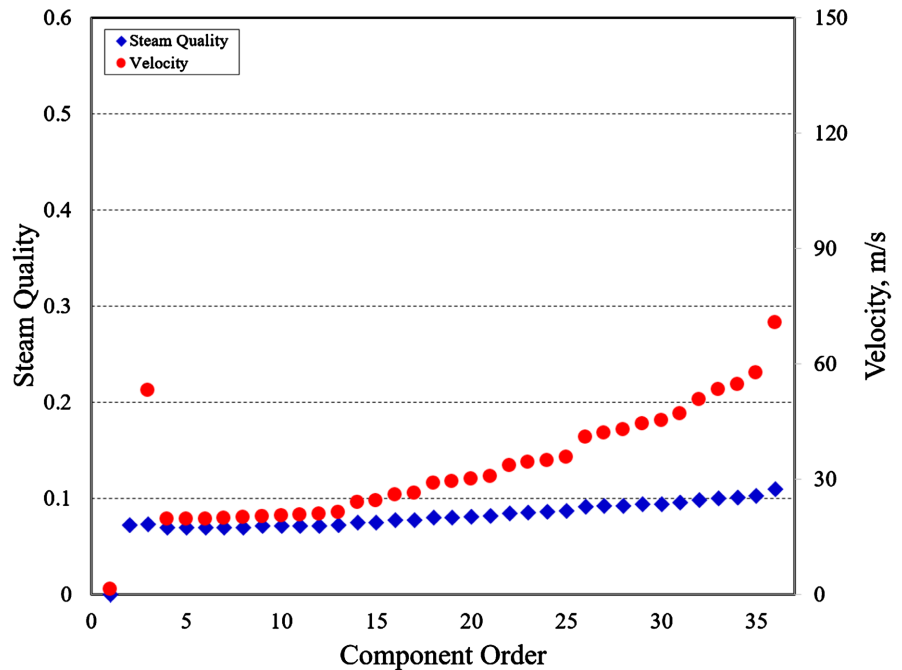


Figure 4. Steam quality and velocity by component order for Case 1.

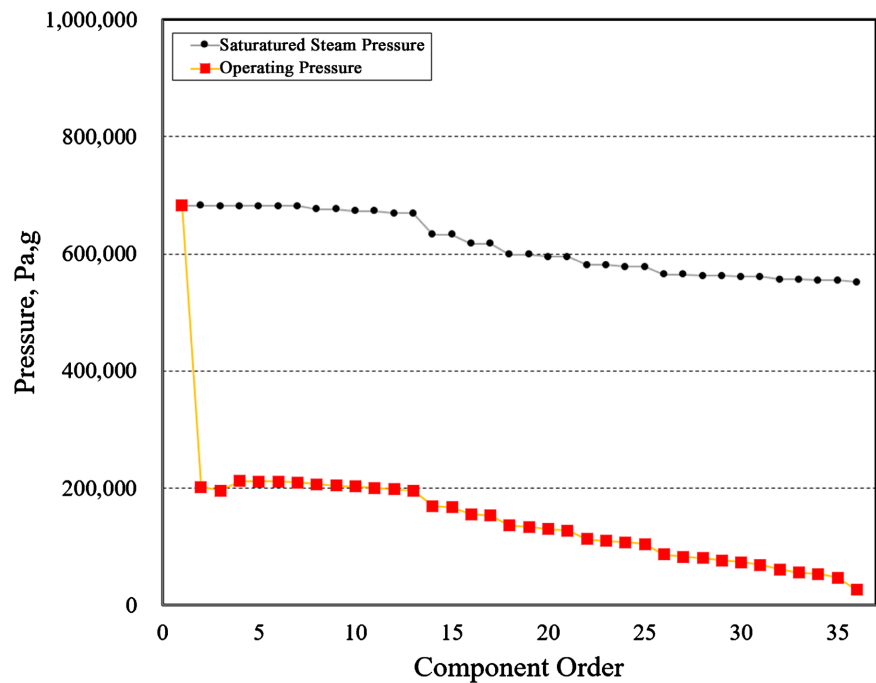


Figure 5. Operating and saturated vapor pressure by component order for Case 1.

phenomenon occurs in the pipeline.

Figure 6 shows the steam quality and flow velocity inside the individual components constituting the pipeline as the analysis results for Case 2. **Figure 7** shows the operating pressure and saturated vapor pressure. Here, the pipeline where the valve is installed is not shown in the graph for comparison with Case

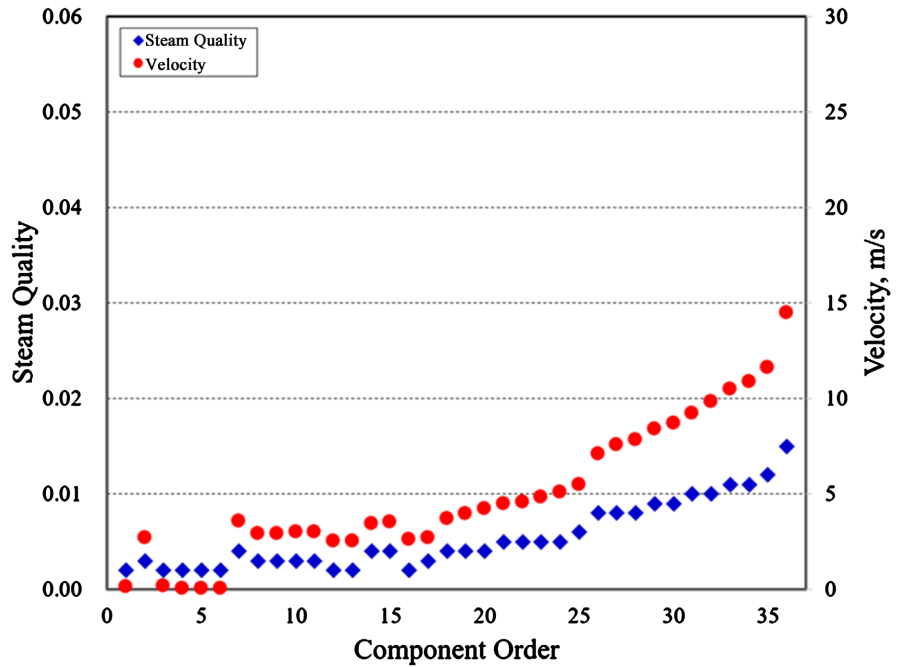


Figure 6. Steam quality and velocity by component order for Case 2.

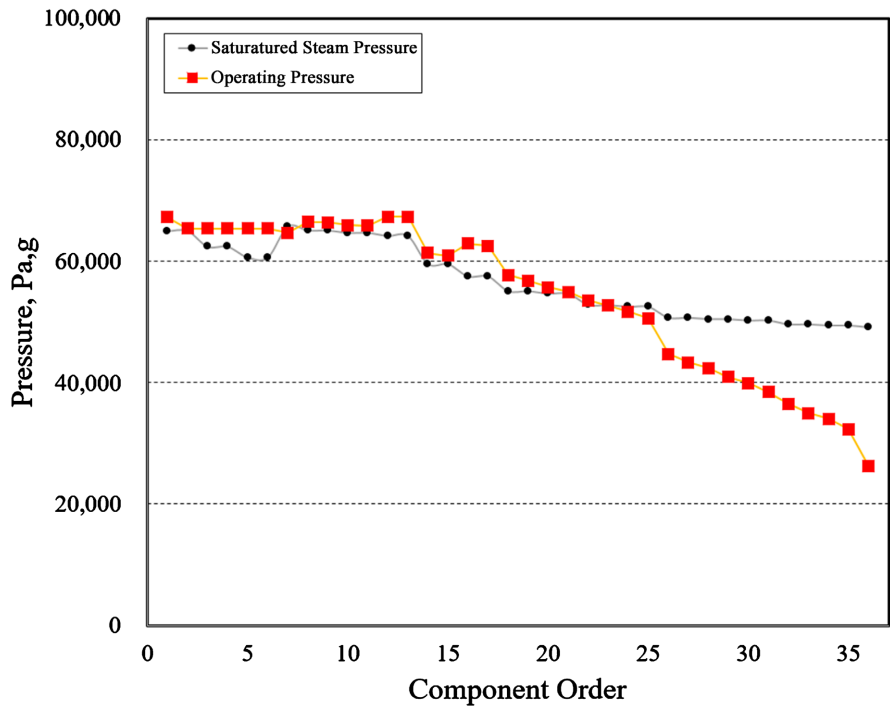


Figure 7. Operating and saturated vapor pressure by component order for Case 2.

1. As shown in **Figure 5**, it can be seen that the steam quality increases as it goes downstream of the pipeline and the flow velocity increases accordingly, even though the increases in the steam quality and flow velocity are smaller than Case 1 during the normal operation. In **Figure 7**, the pressure is maintained higher than the saturated vapor pressure and; from the 23rd component in **Figure 3**, however, the operating pressure decreases below the saturated vapor pressure. From this fact, it can be seen that flashing occurs even in low power conditions during plant startup and shutdown.

3.2. Cause Analysis Using FLUENT

After modeling the pipeline using the FLUENT code, a computational fluid dynamics (CFD) analysis was performed. The reason why the CFD analysis was performed with FLUENT was to verify the results of the ToSPACE analysis described above and to understand the flow behavior inside the pipeline in detail. The analysis model ranges from the pipes upstream of the orifice and valve to the bend and straight pipe of downstream after the two lines are combined. The valve was excluded from the model because it was under the full-open condition. **Figure 8** shows the grid composition of the analysis model. The number of grids was 250,000 of tetrahedral type, and the grids were more densely formed at the part where the fluid was combined.

The inlet boundary conditions used in the analysis are the same as those presented in **Table 1**. However, since the end of the pipeline was not modeled in the CFD analysis using FLUENT, the ToSPACE analysis results at the same location were applied. The turbulence viscosity model was applied with the RNG k- ϵ model. In this analysis, only the flow distribution and pressure change were identified, so the energy balance was not calculated assuming that the temperature

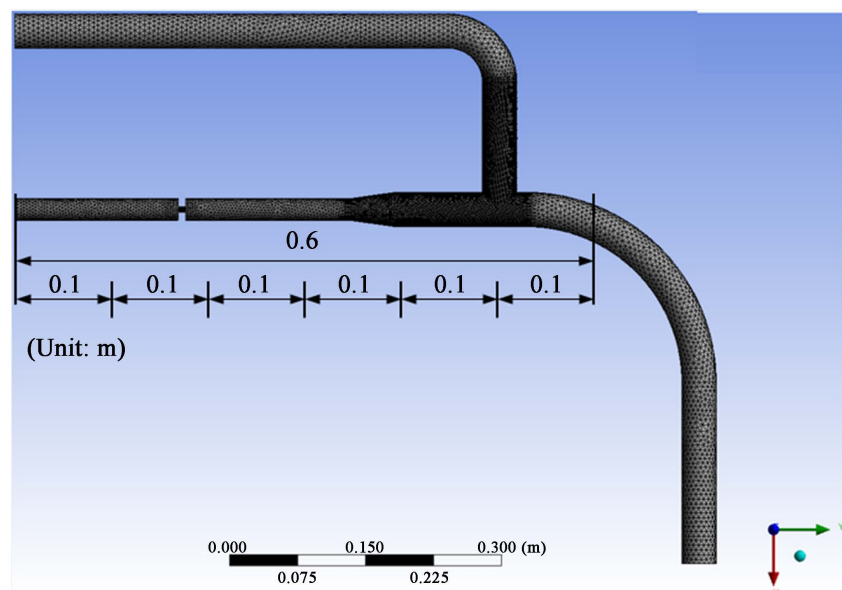


Figure 8. Analysis model and grid composition for fluid dynamic analysis using FLUENT code.

of the fluid was uniform. The CFD analysis was also performed for two cases. **Figure 9** shows the streamline distribution as a result of the analysis of Case 1, where the fluid flows only through the orifice line. As shown in the figure, fast flow is formed at the downstream of the orifice, and a turbulence penetration occurs along the pipeline in which fluid does not flow. **Figure 10** shows the distribution of operating pressure extracted at the centerline from the inlet of the orifice

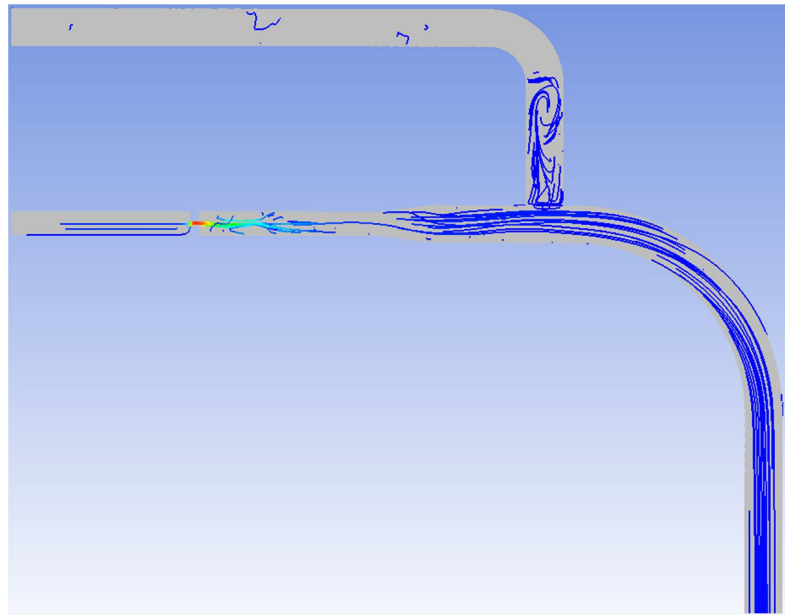


Figure 9. Streamline distribution for Case 1.

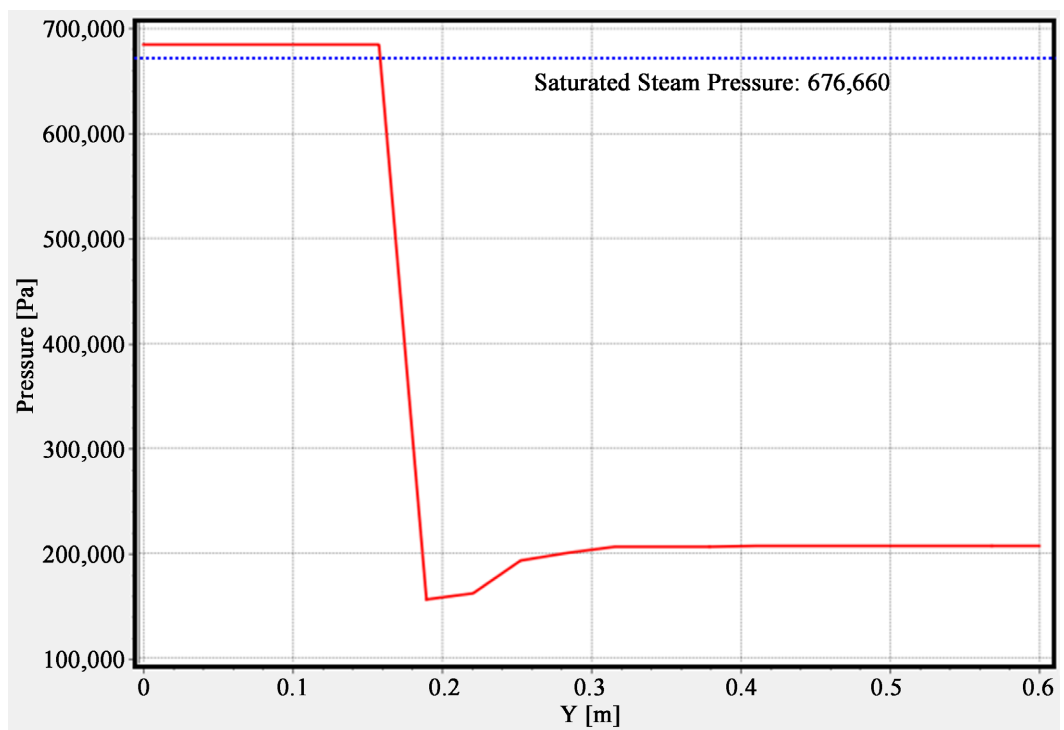


Figure 10. Operating and saturated vapor pressure by distance for Case 1.

to the bend (see **Figure 8**) with the saturated vapor pressure at the outlet temperature (169°C). As can be seen from the figure, after passing the orifice, the pressure rapidly decreases below the saturated vapor pressure. This is similar to the result analyzed using ToSPACE in **Figure 5**.

Figure 11 shows the velocity vector distribution as the result of the analysis of Case 2 where the fluid flows through both pipelines. It can be seen that the fluid passing the orifice is somewhat stagnant due to the fast flow in the upper pipeline. **Figure 12** shows the pressure distribution from the inlet of the orifice to the

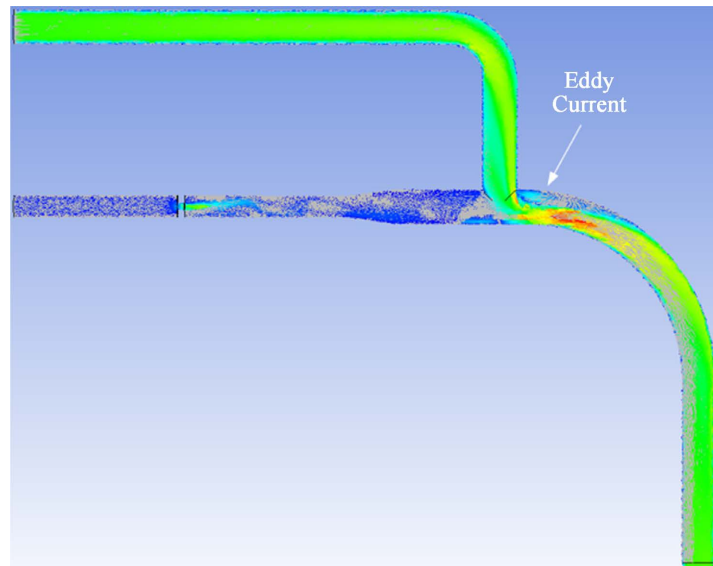


Figure 11. Vector distribution for Case 2.

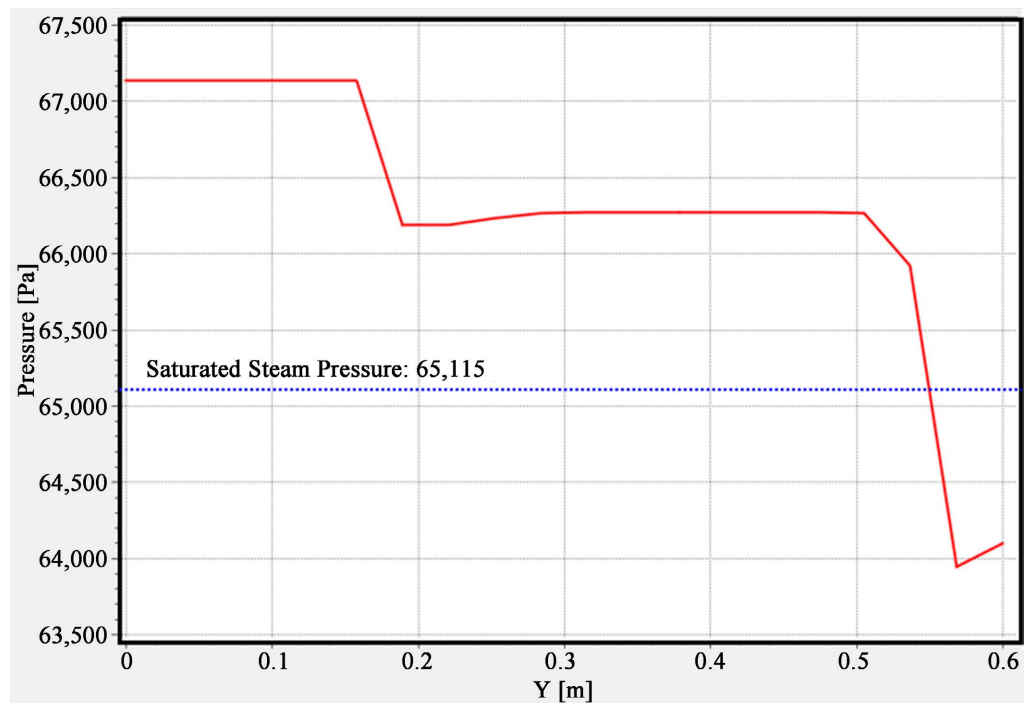


Figure 12. Operating and saturated vapor pressure by distance for Case 2.

bend (see **Figure 8**) with the saturated vapor pressure at the outlet temperature (114°C). As shown in the figure, the operating pressure of the fluid passing the orifice is maintained above the saturated vapor pressure due to the fast flow in the upper pipeline and then, after the flow of the two pipelines is merged, the pressure rapidly drops below the saturated vapor pressure at a position of about 0.55 m (rear end of the sixth component of ToSPACE in **Figure 3**) due to the effects of flow separation and secondary flow.

3.3. Theoretical Analysis for Cavitation and Flashing

As with ToSPACE and FLUENT analyses, likelihood of cavitation and flashing was assessed for two cases: fluid flows only through the orifice pipeline (Case 1) and fluid flows through both the valve and orifice pipelines (Case 2). For this evaluation, Tullis model [5] [6] was applied. The Tullis model does not evaluate the potential of cavitation and flashing as a quantitative value, but evaluates the intensities of cavitation occurrence. It can be calculated from Equations (1) to (4) below.

$$\sigma_i = 0.62 + 4.4C_d + 6.6C_d^2 + 1.3C_d^3 \quad (1)$$

$$\sigma_c = 0.78 + 1.0C_d + 7.9C_d^2 + 3.2C_d^3 \quad (2)$$

$$\sigma_{id} = -0.11 + 6.5C_d - 7.6C_d^2 + 8.6C_d^3 \quad (3)$$

$$\sigma_{ch} = 0.15 + 1.2C_d - 0.31C_d^2 + 3.3C_d^3, \quad (4)$$

where, C_d and β are the same as in Equations (5) and (6).

$$C_d = 0.019 + 0.083\beta - 0.203\beta^2 + 1.35\beta^3 \quad (5)$$

$$\beta = \frac{d}{D}, \quad (6)$$

where, d and D mean the orifice size and the inside pipe diameter, respectively. Equations (7) to (10) show the adjusted cavitation indices, which are compared with the cavitation index (σ) of Equation (11) to determine the intensity of cavitation occurrence.

$$\sigma_{adj,i} = SSE \cdot PSE \cdot (\sigma_i - 1) + 1 \quad (7)$$

$$\sigma_{adj,c} = SSE \cdot PSE \cdot (\sigma_c - 1) + 1 \quad (8)$$

$$\sigma_{adj,id} = SSE \cdot PSE \cdot (\sigma_{id} - 1) + 1 \quad (9)$$

$$\sigma_{adj,ch} = SSE \cdot PSE \cdot (\sigma_{ch} - 1) + 1 \quad (10)$$

$$\sigma = \frac{P_o - P_v}{\Delta P}, \quad (11)$$

where, P_o , P_v and ΔP mean the downstream pressure of orifice, saturated vapor pressure, and pressure difference.

Hence, SSE and PSE represent size scale effect and pressure scale effect. And the cavitation strength is determined by Equations (12) to (16). If the flow condition inside a pipeline is under the condition where cavitation is evaluated to

occur and the operating pressure at the end of the pipeline is less than the saturated vapor pressure, it is determined that flashing could occur.

$$\sigma_{adj,i} < \sigma \quad \text{No Cavitation} \quad (12)$$

$$\sigma_{adj,c} < \sigma < \sigma_{ad,i} \quad \text{Incipient Cavitation} \quad (13)$$

$$\sigma_{adj,id} < \sigma < \sigma_{ad,c} \quad \text{Constant Cavitation} \quad (14)$$

$$\sigma_{adj,ch} < \sigma < \sigma_{ad,id} \quad \text{Incipient Damage} \quad (15)$$

$$\sigma < \sigma_{adj,ch} \quad \text{Chocking.} \quad (16)$$

The temperature and pressure calculated by ToSPACE were used as the input values for cavitation and flashing evaluation. Input values for cavitation and flashing evaluation are presented in **Table 2**. The cavitation and flashing evaluation results are presented in **Table 3**. Both Case 1 and Case 2 were evaluated as Chocking because σ is less than $\sigma_{adj,ch}$. In addition, both Case 1 and Case 2 were evaluated as Flashing because both the downstream pressure of the orifice and the final end pressure of the pipeline are smaller than the saturated vapor pressure.

4. Conclusions

A study was conducted to analyze the cause of wall thinning in the MSR drain pipe of a nuclear power plant in Korea. ToSPACE and FLUENT codes and a theoretical evaluation method were applied to the analysis on causes of the wall thinning. The two cases were analyzed: (Case 1) normal operation condition in

Table 2. Input values for cavitation and flashing evaluation.

Items	Unit	Case 1	Case 2
Temperature	°C	169.56	114.34
Upstream pressure	kPa	682.70	67.21
Downstream pressure	kPa	264.35	50.57
Pressure drop	kPa	487.28	1.83
Final end pressure	kPa	26.19	26.19
Saturated vapor pressure	kPa	682.55	65.00

Table 3. Cavitation and flashing evaluation results.

Items	Case 1	Case 2
σ	0.0012	0.1801
$\sigma_{adj,i}$	1.1142	1.1142
$\sigma_{adj,c}$	0.9604	0.9604
$\sigma_{adj,id}$	0.8629	0.8131
$\sigma_{adj,ch}$	0.2702	0.2702
Evaluation result	Chocking and Flashing	Chocking and Flashing

which the fluid flows only through the pipeline installed with the orifice and (Case 2) lower power condition in which the fluid flows through both pipelines installed with the valve and orifice. As the result of the thermal hydraulic analysis using ToSPACE, it was evaluated that flashing can occur in the both cases because the operating pressures in both cases are lower than the corresponding saturated vapor pressures, the reduced pressures are not recovered over the saturated vapor pressures, and the flow velocities due to the increase of steam quality are increased. The results of the computational fluid dynamics analysis using FLUENT also show that in the both cases, the operating pressures decrease below the saturated vapor pressures. In the cavitation and flashing evaluations with the Tullis model, it was disclosed that choking cavitation and flashing occur in the conditions of the both cases.

As a result, since the pipe location with severe wall thinning is the end of the pipeline entering the condenser, flashing phenomenon by the high-velocity two-phase fluid was evaluated as the cause of the wall thinning in the MSR drain pipes. The wall thinning of the MSR drain pipes replaced with low alloy steel will be monitored continuously. Furthermore, the results of this study will contribute to establishing appropriate design changes in the event of pipe wall thinning in the future.

Conflicts of Interest

The authors declare no conflicts of interest regarding the publication of this paper.

References

- [1] EPRI (2004) Recommendations for Controlling Cavitation, Flashing, Liquid Droplet Impingement, and Solid Particle Erosion in Nuclear Power Plant Piping Systems, 1011231, Final Report.
- [2] Hwang, K.M., Seo, H.K., Lee, C.K. and Nam, W.C. (2017) Development of LDIE Prediction Theory in the Condition of Magnetite Formation on Secondary Side Piping in Nuclear Power Plants. *World Journal of Nuclear Science and Technology*, *7*, 1-14. <https://doi.org/10.4236/wjnst.2017.71001>
- [3] Hwang, K.M., Lee, D.J., Yun, H., Yoo, S.C. and Kim, J.H., (2022) Analysis of Material Loss Behavior According to Long-Term Experiments on LDIE-FAC Multiple Degradation of Carbon Steel Materials. *World Journal of Nuclear Science and Technology*, *12*, 1-10. <https://doi.org/10.4236/wjnst.2022.121001>
- [4] Hwang, K.M., Yun, H., Seo, H.K., Lee, G.Y. and Kim, K.W. (2019) Development of ToSPACE for Pipe Wall Thinning Management in Nuclear Power Plants. *World Journal of Nuclear Science and Technology*, *9*, 1-15. <https://doi.org/10.4236/wjnst.2019.91001>
- [5] EPRI (1993) A Method to Predict Cavitation and the Extent of Damage in Power Plant Piping—Tier 1: Cavitation Erosion Model, TR-103198-T1, Final Report.
- [6] EPRI (1993) A Method to Predict Cavitation and the Extent of Damage in Power Plant Piping—Tier 2: Cavitation Coefficients, TR-103198-T2, Final Report.